Vol. 44, No. 2 (2022) 221-229, DOI: 10.24874/ti.1101.04.21.09

Tribology in Industry

www.tribology.rs

RESEARCH

Optimization of Plasma Spraying Parameters with Respect to Shear Adhesion Strength of Cr3C2-NiCr Coating on 16Mn Steel

Dang Xuan Thao[a], Hoang Van Got[b], Pham Duc Cuong[c,*]

[a]*Faculty of Mechanical Engineering, Hanoi University of Industry, Hanoi City, Vietnam,*
[b]*National Research Institute of Mechanical Engineering, Hanoi City, Vietnam,*
[c]*HaUI Institute of Technology, Hanoi University of Industry, Hanoi City, Vietnam.*

Keywords:

Plasma spraying
Cr_3C_2-NiCr
Coating
Shear adhesion
16Mn steel
Optimization

* Corresponding author:

Pham Duc Cuong
E-mail: phamcuong@haui.edu.vn

Received: 29 April 2021
Revised: 8 June 2021
Accepted: 11 September 2021

A B S T R A C T

The adhesion strength of the thermally sprayed coatings plays a decisive role in the service life of coated parts, especially those working in high temperature environments. Besides factors relevant to material properties, the parameters in the spraying process significantly affect the adhesion strength of the coatings. This paper presents the result of optimizing 3 parameters of atmospheric plasma spraying (APS) including plasma current intensity, powder feed rate and stand-off distance to the shear adhesion strength of the Cr_3C_2-30%NiCr coating on the 16Mn steel achieved the best. The experiments are carried out based on Central Composite Design with 20 trials. Analysis of variance (ANOVA) and genetic algorithm (GA) were used to optimize and evaluate the influences of 3 spraying parameters on the shear adhesion strength of coating and base steel. A quadratic polynomial model is also developed to predict the shear adhesion strength value based on the parameters. The results reveal that all three parameters have significance to shear adhesion, in which the current intensity is the most influential parameter, followed by the stand-off distance and powder feed rate, respectively. The optimization results showed that with the current of 577.5A, powder feed rate of 31.5g/min and stand-off distance of 167mm, the shear adhesion achieved the best value of about 49.81 MPa. In addition, the verified experimental results have an error of about 1.06%, compared with the optimal value.

1. INTRODUCTION

The Cr_3C_2-NiCr coatings are paid attention by researchers and users due to their many advantages against corrosion and wear, especially, in high temperature environments (up to 900°C) [1]. Cr_3C_2–NiCr coatings could be a suitable substitute to WC-Co coatings, as they demonstrate comparable wear performance under erosive, cavitation, abrasive and sliding wear test conditions. Furthermore, it has been shown that Cr_3C_2–

NiCr coatings with minimal microstructural defects such as pores and cracks have excellent wear resistance [2,3]. The melting temperature of Cr_3C_2-NiCr is high, therefore, the coatings are usually produced by thermal spraying. Thermal spray is often employed to deposit coatings that combat wear and corrosion because the deposition rates are relatively fast and a larger surface area can be coated relatively easily [1]. Among the thermal spray techniques, atmospheric plasma spray (APS) is used to deposit ceramics such as alumina, chromia, or zirconia-based coatings to improve wear resistance of various materials [4-6]. Li and Dinh reported that wear resistance of Cr_3C_2-NiCr coating was raised when content of chromium carbides in the powder was increased as well [7]. At high temperatures where WC-based coatings are not suitable, meanwhile Cr_3C_2-NiCr coatings have been extensively used to minimize wear and corrosion. In this case, NiCr alloy serves as a matrix that improves overall coating integrity and corrosion resistance, while Cr_3C_2 constituent serves as a hard phase that assures wear resistance. These constituents of the coating together effectively resist solid particle erosion, high temperature wear (abrasion, erosion, fretting and cavitation) up to 870°C and hot corrosion [8].

In plasma spraying technique, the factors that contribute to the coating quality are related to the spraying device, material, and spraying conditions, etc. Among these factors, the spraying condition plays a key role to create a coating with high adhesion strength, low wear rate, high microhardness and low porosity [4–6,9-11]. During the spraying process, current intensity has a direct impact on anode, which affects the oscillation of the arc. This, in turn, has a strong influence on the temperature, velocity, and trajectory of the powder particles [9,12]. The significant effect of arc power on the particles and trajectory is also reported by Fincke and Swank, that about 10% of the total particles remain un-melted [13]. Yuyan Wang et al. pointed out that horizontal cracks and pores are probable to appear where the power is too small, while a too high power may cause vertical cracks [10]. Another study also showed that cathode erosion occurs mainly due to the high currents that are beyond the expected value of cathode, affecting the operation of plasma flame during the first few hours [14]. The powder feed rate is also influential to coating formation and quality [4-6,11]. It is reported that the small powder feed rate reduces efficiency of the spraying due to the dispersion and loss, which may make the surface not fully covered. In addition, changes of the rate lead to changes of the temperature and velocity of particles, due to the changes of impact of the particles, resulting in changes of the coating quality, such as the porosity increased, the hardness and adhesion strength of the coating and base metal reduced [11]. For a particular plasma spraying deposition process, the optimum stand-off distance depends on the arc, the plasma gas flow rate, the type and size of the powder particles. At a short spraying distance, a higher particle velocity usually results in lower porosity. Some particles are re-solidified due to cooling while moving at a long distance, resulting in a high porosity and low deposition of the coatings. Fincke et al. found an inverse relationship between porosity and deposition efficiency and the efficiency decreased when spraying distance increased [15]. For each specific material and substrate pair, it is essential to define a set of spraying parameters for high coating quality. According to this approach, many scientists have conducted experimental planning and solve optimization problems to provide mathematical functions representing correlations between spray parameters and coating properties, building predictive models [4-6]. On that basis, the optimal spray parameter sets are proposed so that the coating could achieve the best properties.

This paper, aims at finding the optimal spraying parameters for the highest adhesion strength of the Cr_3C_2-30%NiCr coating on the 16Mn steel substrate. Experimental planning method using the central composite design [16-18] combining with ANOVA [17] and genetic algorithm [16] is applied to evaluate the effect of each parameter on the shear adhesion strength and find the optimization values of the spray parameters with regard to highest shear adhesion of the coating. Besides, the mathematical relationship between the parameters and the shear adhesion strength is established, thereby, designing the coating.

2. MATERIALS AND METHODS

2.1. Preparation of steel substrate and coating material

16Mn steel is used for metal substrate because this alloy steel is commonly used in industrial machine parts. Before coating, sample surface is cleaned and roughened by abrasive blasting. The roughness of the sample (Rz ~ 71μm) for best adhesion is given [19]. Cr_3C_2-30%NiCr powder (Sulzer Metco - Singapore) is chosen for use in this study. Cr_3C_2-30%NiCr particles have an average diameter of -30/+5 μm and its chemical composition includes: C ≤ 0.2%, Si ≤ 0.5%, NiCr 29.5% and Cr_3C_2 69.8%.

2.2. Plasma coating system

Plasma spray equipment 3710-PRAXAIR-TAFA (USA), the 1264 powder feeding system that operates on a volumetric feed principle and directly controls the powder feed rate by varying the rotation speed of the disk, and spray gun SG-100 with external powder injection were used in this work. The coating process is carried out as diagram shown in Figure 1.

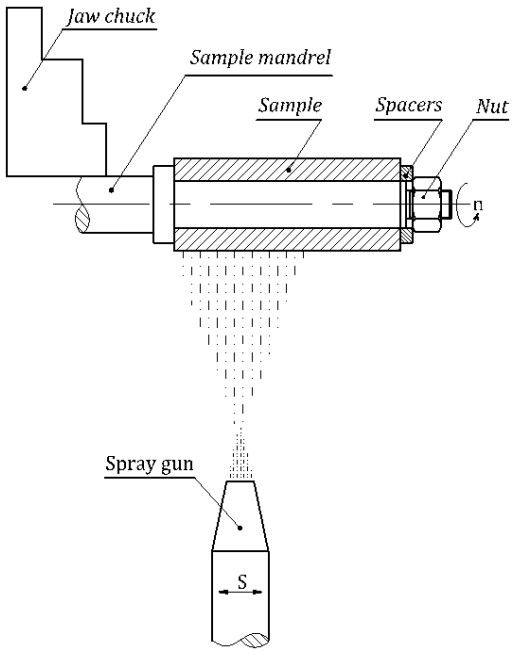

Fig. 1. Diagram of spraying process.

The coating has a minimum thickness of 1000μm with the standard deviation is +100μm. Samples after spraying are cut into small samples, using wire cutter and then ground on a grinder to a height of 8.2mm as shown in Figure 2.

Fig. 2. Sample after coating.

2.3. Measurement system

The shear adhesion strength is determined using a tensile compression tester (Model BESTUTM 500HH, Korea). The measuring samples and measuring procedures are carried out according to JIS H8664-1977 standard with the measurement principal diagram shown in Figure 3. In this study, the coating (with surface area F of 1030mm^2) is separated by the force (P) in a perpendicular direction, as shown in Figure 4. The shear adhesion strength (τ_{Sa}) is defined as:

$$\tau_{Sa} = \frac{P}{F}; \text{ (MPa)} \quad (1)$$

Figure 5 shows the samples including steel substrate and coatings (in the O ring shape) after adhesion the tests.

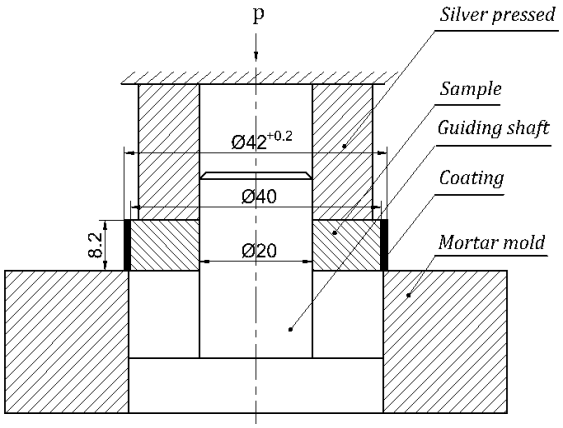

Fig. 3. Diagram for the shear adhesion strength test of the coating.

Fig. 4. Sample holder.

Fig. 5. Coating separated from the base steel

2.4. Experimental matrix and spray parameters

In this study, the experiment was designed according to Central Composite Design method [16-18] with 2^k factorial experiments (coded as -1 and +1), 6 central points (coded as 0) and 2k axial points (placed at -α and +α, where ($\alpha = \sqrt[4]{2^3} = 1.682$)) [20]. The values of each input at all the levels are shown in Table 1.

Table 1. Levels of parameters.

Parameters	Symbols	Unit	Levels				
			-α	-1	0	1	+α
Current intensity	I_s	A	381.82	450	550	650	718.18
Powder feed rate	m_s	g/min	13.18	20	30	40	46.82
Stand-off distance	L_s	mm	92.73	120	160	200	227.27

For spraying experiments, the current intensity (I_s), powder feed rate (m_s) and stand-off distance (L_s) were changed in each trial as shown in Table 2. Other spraying parameters were kept constant, including the power of 35V, Ar gas flow P_{Ar} = 50 liters/min, H_2 gas flow P_{H2} = 5 liters/min, and injection angle of 90°.

3. RESULT AND DISCUSSION

The process of spray coating on the samples is carried out according to Table 2. The results of measuring the adhesion strength of each experiment is the average of 3 measured samples which are also presented in this Table 2.

Table 2. Experiment matrix and result.

No.	Parameters			Results
	I_s (A)	m_s (g/min)	L_s (mm)	τ_{Sa} (MPa)
1	550	30	160	49.9
2	650	40	120	45.2
3	550	30	160	48.0
4	650	20	120	41.6
5	650	40	200	44.0
6	450	40	120	43.1
7	550	30	160	51.7
8	550	30	92.73	38.2
9	550	46.82	160	43.6
10	550	30	227.27	42.8
11	450	20	200	41.6
12	718.18	30	160	44.0
13	550	30	160	48.8
14	450	20	120	36.3
15	550	30	160	49.7
16	650	20	200	46.1
17	550	13.18	160	40.2
18	550	30	160	48.5
19	381.82	30	160	38.8
20	450	40	200	43.5

Table 3. ANOVA results of shear adhesion strength.

Source	Degree Freedom (DF)	Sum squared deviation (Seq SS)	Contribution to the model	Average squared (Adj MS)	Statistical value (F-Value)	Probability value (P-Value)
Model	9	317.923	93.85%	35.325	16.96	0.000
Linear	3	71.803	21.20%	23.934	11.49	0.001
I_s	1	32.740	9.66%	32.740	15.72	0.003
m_s	1	18.553	5.48%	18.553	8.91	0.014
L_s	1	20.510	6.05%	20.510	9.85	0.011
Square	3	224.874	66.38%	74.958	35.99	0.000
I_s*I_s	1	57.832	17.07%	85.699	41.14	0.000
m_s*m_s	1	57.519	16.98%	73.723	35.39	0.000
L_s*L_s	1	109.523	32.33%	109.523	52.58	0.000
Interaction	3	21.245	6.27%	7.082	3.40	0.062
I_s*m_s	1	6.480	1.91%	6.480	3.11	0.108
I_s*L_s	1	0.720	0.21%	0.720	0.35	0.570
m_s*L_s	1	14.045	4.15%	14.045	6.74	0.027
Error	10	20.829	6.15%	2.083		
Lack-of-Fit	5	12.076	3.56%	2.415	1.38	0.366
Coefficient of determination R^2: 93.85%; Adjusted coefficient of determination R^2(adj): 88.32%						

3.1. Contribution of parameters on shear adhesion strength

The ANOVA results of the shear adhesion strength are introduced in Table 3. It is revealed that: In the linear model, the current intensity is the most influential (9.66%/21.20% of the contribution), followed by the stand-off distance (6.05%/21.20%) and powder feed flow is the last (5.48%/21.20%). Similar findings were reported by Manjunath et al [6] although the coating material, outputs and the optimization method were different.

When considering the influence of single factors and the interaction between them, the analysis results show that all factors have an influence on the shear adhesion strength of the coating to the steel substrate. Among them, the Ls*Ls was the most influential (32.33%). Figure 6 shows the influence of Is, ms, and ls on the shear adhesion.

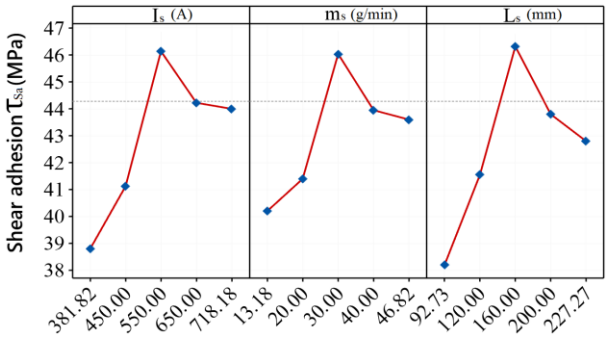

Fig. 6. Influence of parameters on shear adhesion strength.

It is seen from the figure that the shear adhesion increases with increasing Is from 381.82 to 550A. When increasing I_s, working temperature also increases, leading to an increase in the melting of the particles. As a result, the shear adhesion increases accordingly and reaches highest value at Is of about 550A. However, continuing to increase the Is, shear adhesion tends to decrease. This can be explained by considering the fact that at high temperatures (i.e., Is > 550A), small particles are possibly burned and oxidized, thereby reducing the adhesion strength of the coating to the substrate.

In the case of powder feed rate (ms), the shear adhesion increases when increasing the m_s from 13.18 to 30g/min. Then, it decreases when ms is further increased. This can be explained by considering the relation between number of spraying particles and their state during travelling to substrate. With low ms (13.18g/min), particles may easily be burned and oxidized, leading to the low shear adhesion. Increasing ms, the oxidation of particles possibly reduces, leading to increased adhesion. However, with high m_s (> 30g/min), increased number of spray particles to an extent that some particles may not be completely melted, resulting in reduced adhesion to the surface.

Regarding stand-off distance (Ls), when increasing Ls from 92.73mm to 160mm, the adhesion strength increases. However, if we continue to increase Ls above 160mm, the adhesion strength will decrease. This can be explained on the basis of kinetic energy and state of the particle when it collides with the ground surface. At a close distance (92.73mm), the beam of molten particles strongly collides with the substrate and can be deformed greatly, affecting the coating structure and reducing the adhesion to the substrate. Increasing Ls will reduce the impact of molten particles and increase the adhesion. However, when Ls > 160mm, some particles can be reduced in temperature and solidified again. In addition, the kinetic energy of the particles when hitting the substrate is reduced, leading to a decrease in the adhesion strength.

To understand the interaction between the factors, an interaction matrix diagram is built as shown in Figure 7. The diagram illustrates the influence of the input parameters on the shear adhesion strength. Observation shows that the effect of the input parameters on the output parameters is complex. The following analysis further clarifies this situation:

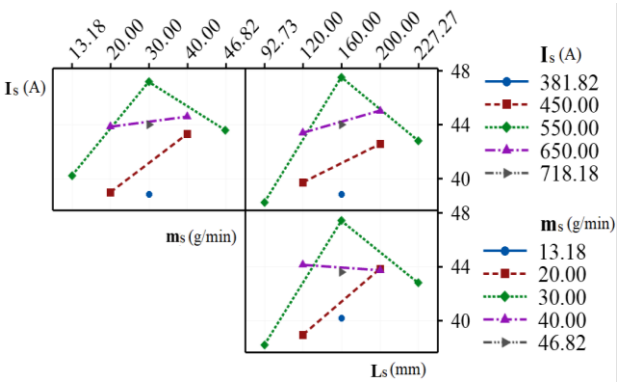

Fig. 7. Influence of interaction between parameters on shear adhesion strength.

Analysis of the impact between the current intensity and powder feed rate reveals that: When the current intensity was 550A and the powder feed rate increased from 13.18 to 30g/min, the shear adhesion strength went up. However, since the powder feed rate increased from 30 to 46.82g/min, the shear adhesion strength went down. In each case of 450A and 650A of I_s, an increase of the powder supply flow from 20 to 40 g/min resulted in an increase of the adhesion strength. However, the influence of m_s on the shear adhesion strength is greater in the case of 450A of I_s than 650A. This can be explained by the fact that when the current intensity is raised, the power of the arc increases. Then, the particles that are in a good molten condition achieve high deposition. The higher powder feed rate into the spraying area causes the lower temperature for the particle melting due to heat dissipation by the number of particles. This can also reduce the impact force of particles with the substrate resulting in a decrease in the shear adhesion. In order to improve the spraying effectiveness while increasing the powder feed rate, it is necessary to continue to increase the current intensity for a higher temperature of particle melting, however, this improvement is not probably effective.

Analyzing the influence between the current intensity and stand-off distance also indicates that: At 550A of a current intensity, the shear adhesion strength was improved as the spraying distance was changed from 92.73 to 160mm. However, it decreased as stand-off distance was continually increasing. The shear adhesive strength increases as the stand-off distance increases from 120 to 200mm at both 450A and 550A of the current intensity. However, the influence of stand-off distance on the strength at 450A was greater than 650A. This can be explained that: the increase of spraying distance leads to re-solidification of the particles due to cooling (the smaller the particles, the faster the re-solidification), at the same time, more oxidized particles cause an increase to coating porosity and decrease to the shear adhesion strength. On the other hand, the short distance limits the spraying effectiveness owing to the strong impact force causing the particles to be thrown out.

The interaction between the powder feed rate and the stand-off distance shows that: at 30g/min of the powder feed rate, the shear adhesion strength was improved as the spraying distance was turned from 92.73 to 160mm. However, it was reduced when stand-off distance was continually growing up from 160 to 227.27mm. At both 20g/min and m_s = 40g/min of the powder feed rate, the shear adhesion strength increases as the spraying distance increases from 120 to 200 mm. However, the influence of powder feed rate on the shear adhesion strength was considerably higher at 20g/min than 40g/min of the powder feed rate. This can be explained that: to achieve higher shear adhesion strength, the spraying distance must increase while the powder feed rate must decrease. The heat goes up due to the reduction in particle density, however, the distance increased leads to appropriate thermal efficiency at the time of impact for the highest shear adhesion strength. On the contrary, the powder feed rate is too high causing the temperature to go down, the particle velocity also decreases and as a result, the quality and shear adhesion strength of the coating to decrease accordingly. In short, the stand-off distance must be reduced as the powder feed rate is high.

3.2. Regression model of adhesion strength determination

The tests are performed according to table 2, the value of τ_{Sa} at each trial is also included in this table. The ANOVA is applied to build adhesion strength model. And a quadratic polynomial regression model that was the suitable model to predict the adhesion strength as by Eq. (2):

$$\begin{aligned}\tau_{Sa} = {} & -143.1 + 0.3227\, I_s + 2.498\, m_s + 0.723\, L_s \\ & - 0.000244\, I_s{*}I_s - 0.02261\, m_s{*}m_s - 0.001723\, L_s{*}L_s \\ & - 0.000900\, I_s{*}m_s - 0.000075\, I_s{*}L_s - 0.00331\, m_s{*}L_s\end{aligned} \quad (2)$$

The ANOVA results for τ_{Sa} are presented in Table 3. First, in the Lack-of-Fit section, the P-value is much greater than the significance level. This means that the model is well suited to the data. Second, considering the individual component values of the regression model (Linear, Square and Interaction) reveals that their P-values are relatively small (less than < 0.05; statistically significant). In other words, the presence of each component is of high significance in the regression model [20]. The regression coefficient (R^2) shows that 93.85% of the experimental data fit the predicted data from the model. R^2(adj) = 88.32% are reasonable as well.

Regression model is applied to predict the shear adhesion, the results of the comparison between the predicted and experimental shear adhesion strength are introduced in Table 4 and described in Figure 8.

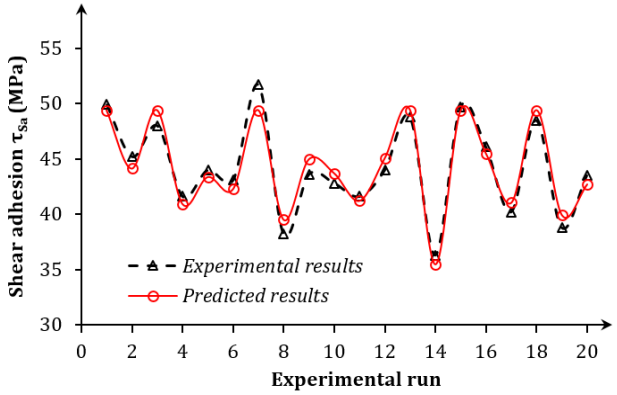

Fig. 8. The predicted and experimental results of shear adhesion strength.

Table 4. Comparison between the predicted and experimental results.

No.	Experimental results	Predicted results	Difference (%)
1	49.9	49.4	1.0
2	45.2	44.1	2.4
3	48.0	49.4	2.9
4	41.6	40.9	1.6
5	44.0	43.4	1.5
6	43.1	42.3	1.9
7	51.7	49.4	4.5
8	38.2	39.5	3.4
9	43.6	45.0	3.1
10	42.8	43.7	2.1
11	41.6	41.2	0.9
12	44.0	45.1	2.4
13	48.8	49.4	1.2
14	36.3	35.5	2.3
15	49.7	49.4	0.6
16	46.1	45.5	1.4
17	40.2	41.0	2.1
18	48.5	49.4	1.9
19	38.8	39.9	2.9
20	43.5	42.7	1.8
Average difference			2.1

The results indicate that the predicted shear adhesion strength is nearly close to the measured shear adhesion with 4.5% of the maximum difference and 2.1% of the average difference. Thus, the regression model is tested and able to be applied for predicting the shear adhesion strength as well as optimizing it.

3.3. Optimization result for shear adhesion strength

The Minitab 19™ software is applied to solve the model optimization problem with the goal of obtaining the highest adhesion strength within specific conditions. Results are shown in Figure 9.

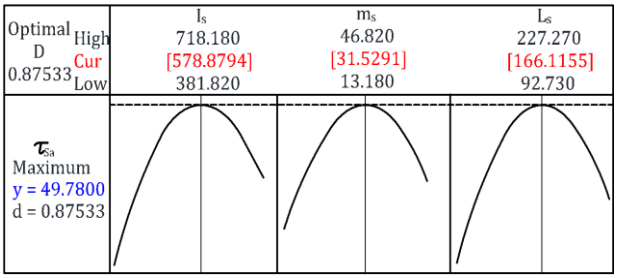

Fig. 9. Graphs showing relationship of spraying parameters and shear adhesion strength.

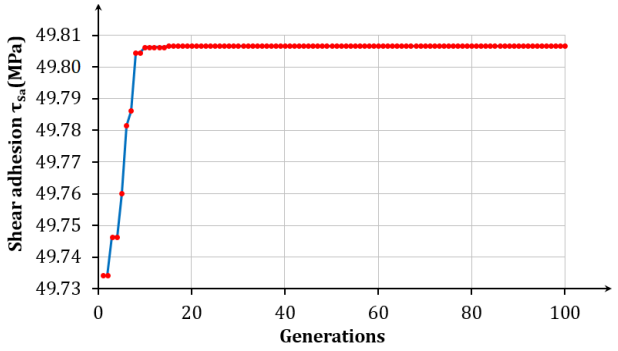

Fig. 10. Optimization results using GA.

In addition, the genetic algorithm (GA) is used with the following parameters: 100 of population, 0.25 of crossover probability, 0.05 of mutation probability and 4 of mutation parameter. The result of solving the optimization problem is presented in Figure 10.

The results of solving the problem with the goal of the shear adhesion strength using two methods are shown in Table 5. It can be said that the two methods provided similar outcomes (the largest difference is 0.6%). Thus, this set of parameters is the optimal values to achieve the maximum value of shear adhesion strength of coating on base steel.

Table 5. Optimal spraying parameters for maximum shear adhesion strength according to GA.

Solution	I_s	m_s	L_s	τ_{Sa} (Fit)
ANOVA	578.9	31.5	166.1	49.78
GA	577.5	31.5	167.0	49.81
Difference (%)	0.24	0.00	0.6	0.06

3.4. Examination of optimal parameters for shear adhesion strength according to GA

To verify the optimized spraying parameters, the experiment for examining the parameters defined according to GA is conducted with I_s = 577.5A; m_s = 31.5g/min and L_s = 167mm. It is performed with 5 samples and its results are presented in Table 6 demonstrate that the value predicted by GA and experimented are consistent (1.06% of difference). In short, these spraying parameters represent the reliable optimization outcome for the highest shear adhesion strength.

Table 6. Measurement results on samples for examining optimization.

Samples	1	2	3	4	5	τ_{Sa} (Average)
Measurement results	49.86	50.05	49.64	48.5	48.36	49.28 MPa)

4. CONCLUSION

In this work, Cr_3C_2-30%NiCr coatings were created on 16Mn steel substrate by atmospheric plasma spraying. 3 parameters of the plasma spraying process including plasma current intensity, powder feed rate, and stand-off distance were studied and optimized using central composite design combining with ANOVA and Genetic Algorithm with respect to the shear adhesion strength of the coating. The results are summarized as follows:

- The current intensity (I_s) has the greatest influence on the shear adhesion strength of the Cr_3C_2-30%NiCr coating on the 16Mn steel sample, followed by the stand-off distance (L_s) and the powder feed rate (m_s), respectively.
- Applying the ANOVA method, the optimal values of the spraying parameters were: I_s = 578.9A, m_s = 31.5g/min and L_s = 166.1mm, along with the maximum achievable value of shear adhesion strength was 49.78MPa. On the other hand, the optimized results obtained using Genetic Algorithm were: I_s = 577.5A, m_s = 31.5g/min and L_s = 167.0mm, whereas the shear adhesion strength of coating was predicted to be 49.81MPa. It is concluded that the two methods provided similar outcomes.
- The shear adhesion strength obtained from verification test was 49.28MPa, which is about 1.06% less than the optimal prediction result. It is confirmed that the optimal spray parameters can be used to achieve the good coating quality along with the maximum of enhanced shear adhesion strength.

Acknowledgments

Financial support from the Hanoi University of Industry for this research is acknowledged with gratitude.

REFERENCES

[1] D. Tejero-Martin, M. Rezvani Rad, A. McDonald, T. Hussain, Beyond traditional coatings: a review on thermal-sprayed functional and smart coatings, Journal of Thermal Spray Technology, vol. 28, iss. 4, pp. 598–644, 2019, doi: 10.1007/s11666-019-00857-1

[2] V. Matikainen, G. Bolelli, H. Koivuluoto, P. Sassatelli, L. Lusvarghi, P. Vuoristo, Sliding wear behaviour of HVOF and HVAF sprayed Cr3C2-based coatings, Wear, vol. 388–389, pp. 57–71, 2017, doi: 10.1016/j.wear.2017.04.001

[3] V. Matikainen, H. Koivuluoto, P. Vuoristo, A study of Cr3C2-based HVOF- and HVAF-sprayed coatings: abrasion, dry particle erosion and cavitation erosion resistance, Wear, vol. 446–447, 2020, Available online, doi: 10.1016/j.wear.2020.203188

[4] N.H.N. Yusoff, M.J. Ghazali, M.C. Isa, A.R. Daud, A. Muchtar, S.M. Forghani, Optimization of plasma spray parameters on the mechanical properties of agglomerated Al2O3-13%TiO2 coated mild steel, Materials and Design, vol. 39, 504–508, 2012, doi: 10.1016/j.matdes.2012.03.019

[5] C.S. Ramachandran, V. Balasubramanian, P.V. Ananthapadmanabhan, Multiobjective optimization of APS process parameters to Yttria-Stabilized Zirconia coatings using Response surface methodology, Journal of Thermal Spray Technology, vol. 20, pp. 590–607, 2011, doi: 10.1007/s11666-010-9604-y

[6] G.C.M. Patel, N.B. Pradeep, L. Girisha, H.M. Harsha, A.K. Shettigar, Experimental analysis and optimization of plasma spray parameters on microhardness and wear loss of Mo-Ni-Cr coated super duplex stainless steel, Australian journal of Mechanical Engineering, Available online, pp. 1–13, 2020, doi: 10.1080/14484846.2020.1808760

[7] J. Li, C. Ding, Improvement in the properties of plasma-sprayed chromium carbide coatings using nickel-clad powders, Surface and Coatings Technology, vol. 130, iss. 1, pp. 15–19, 2000, doi: 10.1016/S0257-8972(00)00678-2

[8] H.P. Thi, T.N. Van, Q.L. Thu, L.P. Thi, T.T. Van, T.D. Bich, C.L. Quoc, Cr_3C_2-25NiCr Cermet Coating: Preparation, PTFE Sealant, Wear and Corrosion Resistances, Journal of Thermal Spray Technology, vol. 30, pp. 716–724, 2021, doi: 10.1007/s11666-021-01155-5

[9] T. Kavka, J. Matějíček, P. Ctibor, A. Mašláni, M. Hrabovský, Plasma Spraying of Copper by Hybrid Water-Gas DC Arc Plasma Torch, Journal of Thermal Spray Technology, vol. 20, pp. 760–774 2011, doi: 10.1007/s11666-011-9633-1

[10] Y. Wang, Y. Han, C. Lin, W. Zheng, C. Jiang, A. Wei, Y. Liu, Y. Zeng, Y. Shi, Effect of spraying power on the morphology of YSZ splat and micro-structure of thermal barrier coating, Ceramics International, vol. 47, iss. 13, pp. 18956-18963, 2021 doi: 10.1016/j.ceramint.2021.03.238

[11] J.R. Davis, Handbook of Thermal Spray Technology, ASM International, Thermal Spray society, 2004.

[12] D. Rigot, G. Delluc, B. Pateyron, J.F. Coudert, P. Fauchais, J. Wigren, Transient evolution and shifts of signals emitted by A DC plasma gun (type PTF4), High Temperature Material Processes, vol. 7, iss. 2, pp. 175-185, 2003, doi: 10.1615/HighTempMatProc.v7.i2.70

[13] J.R. Fincke, W.D. Swank, The effect of plasma jet fluctuations on particle timetemperature histories, in T.F. Bernecki (Ed.), Thermal Spray Coatings: Properties, Processes and Applications, ASM International, pp. 193–198, 1991.

[14] X. Zhou, J. Heberlein, An experimental investigation of factors affecting arc-cathde erosion, Journal of Physics D: Applied Physics, vol. 31, no. 19, pp. 2577–2590, 1998, doi: 10.1088/0022-3727/31/19/031

[15] J. Fincke, W.D. Swank, Air plasma spraying of zirconia: spray characteristics, deposition efficiency and porosity control by standoff distance, in CC. Berndt (Ed.), Proceedings of international thermal spray conference, ASM International, pp. 513–518, 1992.

[16] G.R. Chate, G.C.M. Patel, A.S. Deshpande, M.B. Parappagoudar, Modeling and optimization of furan molding sand system using design of experiments and particle swarm optimization, Proceedings of the Institution of Mechanical Engineers, Part E: Journal of Process Mechanical Engineering, vol. 232, iss. 5, pp. 579–598, 2017, doi: 10.1177/0954408917728636

[17] G.C.M. Patel, P. Krishna, M.B. Parappagoudar, Modelling of Squeeze Casting Process: Conventional Statistical Regression Analysis Approach, Applied Mathematical Modelling , vol. 40, iss. 15-16, pp. 6869–6888, 2016, doi: 10.1016/j.apm.2016.02.029

[18] G.C.M. Patel, A.K. Shettigar, M.B. Parappagoudar. A systematic approach to model and optimize wear behavior of casting produced by squeeze casting process, Journal of Manufacturing Processes, vol. 32, pp. 199–212, 2018, doi: 10.1016/j.jmapro.2018.02.004

[19] P.D. Cuong, D.X. Thao, Effect of surface roughness and plasma current to adhesion of Cr3C2-NiCr coating fabricated by plasma spray technique on 16Mn steel, International Journal of Modern Physics B, vol. 35, no. 14–16, 2021, doi: 10.1142/S0217979221400373

[20] N.V. Du, N.D. Binh, Experimental planning in engineering, Nxb Science Technology, Hanoi, Vietnam, 2011.